Press, New York, (1975).
(10) D. J. Pedder, *Electrocomp. Sci. Tech.*, **2**, 259 (1976).
(11) M. W. Shafer and J. Armstrong, *IBM Tech. Discuss. Bull.*, **20**, No. 11A, 4,633 (1978)..
(12) D. Galizzioli, F. Tantardini and S. Trasatti, *J. Appl. Electrochem.*, **4**, 57 (1974).
(13) D. Galizzioli, F. Tantardini and S. Trasatti, *ibid.*, **5**, 203 (1975)
(14) T. Okamura, *Denki Kagatu*, **41**, 303 (1973)
(15) S. Pizzini, G. Buzzanca, C. Mari, L. Rossi and S. Torchio, *Mater. Res. Bull.* **7**, 449 (1972).
(16) G. Lodi, C. Bighi and C. de Asmundis, *Mater. Chem.*, **1**, 177 (1976).
(17) H. Tamura and C. Iwakura, *Denki Kagatu*, **43**, 674 (1975).
(18) C. Iwakura, H. Tada and H. Tamura, *Electrochim. Acta*, **22**, 217 (1977).
(19) W. A. Gerrard and B. C. H. Steele, *J. Appl. Electrochem.* **8**, 417 (1978).
(20) T. Arikado, C. Iwakura and H. Tamura, *Electrochim. Acta*, **22**, 513 (1977).
21) L. D. Burke, O. J. Murphy, J. F. O'Neill and S. Venkatesan, *J.C.S. Faraday I*, **73**, 1,659 (1977).
(22) L. Burke, O. J. Murphy and J. F. O'Neill, *J. Electroanal. Chem.* **81**, 391 (1977).
(23) G. Lodi, E. Sivieri, A. de Battiste and S. Trasatti, *J. Appl. Electrochem.* **8**, 135 (1978).
(24) S. Trasatti and W. O'Grady, Advances in Electrochemistry and Electrochemical Engineering, H. Gerischer and C. W. Tobias, eds., John Wiley and Sons, New York (1981).
(25) G. Skorinko, A. K. Goel, and F. H. Pollak, *Bull. Amer. Phys. Soc.*, **25**, 363 (1980).
(26) S. Pizzini and L. Rossi, *Z. Naturforsch.*, **26**, 177 (1971).
(27) F. M. Reames, *Mat. Res. Bull.*, **11**, 1,019 (1976).
(28) M. W. Shafer, R. A. Figat, B. Oosen, S. J. Laplace and J. Angilello, *J. Electrochem. Soc.*, **126**, 1,625 (1979).
(29) L. D. Burke and O. J. Murphy, *J. Electroanal. Chem.*, **112**, 39 (1980).
(30) H. A. Kozlowska, B. E. Conway and W. B. A. Sharp, *Electroanal. Chem. and Interfacial Electrochem.*, **43**, 9 (1973).
(31) M. Pourbaix, "Atlas of Electrochemical Equilibria in Aqueous Solutions," p. 343–349 Pergamon Press, London, 1966.

Transition-State Variation in the Solvolysis of Benzoyl Chlorides*

Ikchoon Lee, In Sun Koo, Se Chul Sohn and Hai Hwang Lee

Department of Chemistry, Inha University, Incheon 160 Korea *(Received February 10, 1982)*

Solvolysis reactions of some substituted benzoyl chlorides were studied in ethanol–water, ethanol–trifluoroethanol and methanol–acetonitrile mixtures. Results showed that the reaction proceeds *via* an S_N2 process in which bond formation is more advanced than bond cleavage. Comparison of the two models for predicting transition state variation indicated superior nature of the quantum mechanical model relative to the potential energy surface model.

Introduction

The reaction mechanism for the nucleophilic substitution reaction at a carbonyl carbon has attracted considerable attention. Specifically the mechanisms of solvolysis and nucleophilic subtitution reactions of benzoyl halides have been studied with a view to making a comparison with those of benzyl derivatives; it has been shown that both exhibit the borderline nature of the process[1], but bond-making is important in the former[1a–b] whereas in the latter bond-breaking is important[1c–d] in the transition state. Recently various models for predicting variations in transition state structure have been used in explaining the properties of nucleophilic substitution reactions. Jencks[2] discussed transition state variation with solvent using an extended Grunwald-Winstein[3] equation(1),

$$\log(k/k_0) = mY + lN \quad (1)$$

Harris *et al.*[4] predicted variation of S_N2 transition state of benzyl derivatives using a potential energy surface model[5] and Lee *et al.*[6] applied the similar model to the S_N2 transition state of benzensulfonyl derivatives.

The potential energy surface (PES) model for predicting transition state variation is based on the application of the Hammond postulate[7] and the Thornton's rule[8] to e.g., a reaction of a nucleophile(N) attacking a substrate (RX),

$$N(B) + RX(A) \longrightarrow [N\cdots R\cdots X]^* \longrightarrow N^+-R + X^- \quad (2)$$

On the other hand, Pross and Shaik[9] introduced a quantum mechanical approach to estimating the effect of subtituents on transition state structure in S_N2 reactions. In this model, the reaction complex is described in terms of a wave function built up from a linear combination of reactant configurations. In an S_N2 reaction, (2), a new bond is formed between A and B and a bond within A is borken as a substrate A(RX) is attacked by a nucleophile B(N).

*Taken as Part 14 of the series "Nucleophilic Substitution at a Carbonyl Carbon".

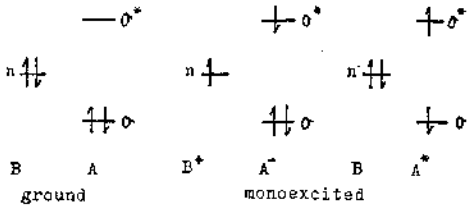

Figure 1. Ground and excited reactant configurations for the description of S_N2 reactions.

Application of the molecular orbital theory to an inter-system perturbation of A by B has been shown to give four main types of interactions[10]; electrostatic, exchange repulsion, polarization and charge-transfer, electron reorganization being involved only in the latter two types of interactions. Since the reaction takes place primarily through the reorganization of the principal reacting electron pairs, Pross and Shaik[9] considered only these two perturbed, together with the ground state, configurations (Figure 1); BA=(N:(R—X)), $B^+A^-=(N^+(R\dot{-}X)^-)$ and BA*=(N:(R—X)*), in which the electron pairs actually involved are those in the frontier orbitals *i.e.*, the nucleophile (a donor) HOMO n and the substrate (an acceptor) σ_{C-X} pair.

The reaction complex along the reaction coodinate is then defined by a wave function, ϕ_i, derived from a linear combination of the three key configurations as in eq. (3).

$$\phi_i=C_1(BA)+C_2(B^+A^-)+C_3(BA^*) \quad (3)$$

The magnitude of coefficient, C_i, reflects the extent of contribution (mixing) of i-th configuration to the wave function. Thus a state (*e.g.* transition state) represented by ϕ_i will reflect and substituent change introduced in B or A by mixing in less of any configuration destabilized by the modification and more of any configurations which are stabilized by the modification.

Let us briefly examine the bonding characteristics of each configuration which contributes to the transition state structure. In the BA configuration, there is no electronic reshuffle, and hence the N···R "no bond" and the R–X bond are involved; structural effect on reaction complex will be a loose N–R and a tight R–X. There is an electron jump from the nucleophile N to an empty orbital, σ^*, of the substrate, RX, in the B^+A^- configuration, and hence the N–R bond is formed while the R–X bond is weakened since the antibonding orbital, σ^*, is occupied; structrual effect will be a tight N–R and a loose R–X bond. Finally in th BA* configuration, one σ electron is promoted into a σ^* orbital within RX, and thus, the N···R "no bond" and the weakened R–X bond will result since both the σ and σ^* of R–X are singly occupied; consequently both the N–R and R–X bonds will become loose. The structural effects of the three key configurations on the reaction complex are summarized in Table 1. Reference to this table enables us to make specific predictions as to how the transition state will change as a result of a given perturbation such as the substituent or the solvent change.

In this work, transition state variation in the solvolysis of some *para*-substituted benzoyl chlorides in EtOH–H_2O, EtOH–TFE and MeOH–MeCN mixtures is investigated applying the extended Grunwald-Winstein equation, (1), the potential energy surface and quantum mechanical models.

TABLE 1: Valence Bond Description of Donor–Acceptor Configurations and Their Structural Effect on the Reaction Complex[9]

Configuration	Valence bond description		Structural effect on reaction complex	
	Primary	Secondary	N–R	R–X
BA	N: R· ·X	N: R⁺ :X⁻	Loose	Tight
B^+A^-	N^+ ·R :X⁻	N^+ R:⁻ ·X	Tight	Loose
BA*	N: R⁺ :X⁻	N: ·R ·X	Loose	Loose

Experimental

GR grade benzoyl chlorides and CF_3CH_2OH(TFE), (Tokyo Kasei), and CH_3OH and C_2H_5OH(Merck) were used without further purification. Water and acetonitrile were used after purification as described in a previous report[11,12]. Kinetic measurements were done conductometrically using the same apparatus and thermostatic bath as before[12]. Pseudo-first order rate constants were determined by Guggenheim method.[13] Rate constants were accurate to ±5 %.

Eesults and Discussion

Substituent and Solvent Effects. Rate constants and activation parameters for solvolysis of parasubstituted benzoyl chlorides obtained in EtOH–H_2O, EtOH–TFE and MeOH–MeCN mixtures are summarized in Tables 2, 3 and 4. It can be seen from Table (2) that the rate constants increase with the more electron-withdrawing substituent and with increasing water content. However Table 3 shows that increasing TFE content of the EtOH–TFE mixture has the effect of increasing the rate constant of the compound with electron-donating substituent (p-CH_3) and of decreasing the rate of those with electron-withdrawing substituent(p-Cl and p-NO_2). This may be considered to result from the greater ionizing power and lower nucleophilicity of TFE compared with ethanol although dielectric constants for the two are similar(26.14 and 24.32 at 25 °C respectively[14]), and is an indication that bond-breaking, which will increase with ionizing power of the solvent, is important with the electron-donating substituent, while bond-making, which will increase with nucleophilicity of the solvent, becomes important with the electron-withdrawing substituent in the transition state. The ΔH^+ values in Table 3 show a general trend of slight increase with the TFE content and with the electron-donating substituent; this again suggests the increase in bond cleavage in the transition state as the TFE content or the electron-donating property of the substituent is increased.

The Hammett plots(Figure 2 and 3) show typical curvature, analogously to hydrolysis of benzyl[4,15] and benzensulfonyl[6,12,16] derivatives. We confirm the importance of bond cleavage in the transition state of the chloride with electron-donating substituent from these plots. Two approximate ρ values (ρ_1 for electron-donating substituent and ρ_2 for

TABLE 2: Rate Constants ($k_1\times10^4$ sec^{-1}) and Activation Parameters for the Solvolysis of *para* Substituted Benzoyl Chlorides in EtOH–H_2O Mixtures at 10 °C, 25° C

Substituents	EtOH (v/v %)	Rate constants 10 °C	Rate constants 25 °C	$\Delta H^{\ddagger}$	$-\Delta S^{\ddagger}$
p-CH_3	100	1.17	5.24	15.9	20
	90	3.27	14.7	16.1	18
	80	6.40	33.0	17.6	11
	70	13.8	75.8	18.2	7
H	100	1.90	7.48	14.5	24
	90	4.27	17.0	14.7	22
	80	6.23	27.7	15.8	17
	70	8.80	39.8	16.1	16
p-Cl	100	3.20	12.1	14.0	25
	90	9.49	32.4	13.0	26
	80	12.9	44.9	13.1	25
	70	15.1	55.9	10.1	25
p-NO_2	100	36.7	135	13.9	20
	90	131	358	10.3	31
	80	180	470	9.8	32
	70	209	580	10.6	29

$\Delta H^{\ddagger}$ in kcal·mole^{-1}. $\Delta S^{\ddagger}$ in e. u

TABLE 3: Rate Constants ($k_1\times10^4$ sec^{-1}) and Activation Parameters for the Solvolysis of *para* Substituted Benzoyl Chlorides in EtOH–TFE Mixtures at 10 °C, 25 °C.

Substituents	EtOH (v/v %)	Rate constants 10 °C	Rate constants 25 °C	$\Delta H^{\ddagger}$	$-\Delta S^{\ddagger}$
p-CH_3	100	1.17	5.24	15.9	20
	80	1.55	7.00	16.1	19
	70	1.77	8.35	16.5	17
	60	2.17	11.2	17.6	13
	50	—	15.4	—	—
H	100	1.90	7.48	14.5	24
	80	1.78	7.20	14.8	23
	70	1.63	6.43	14.6	24
	60	1.43	6.05	15.3	22
	50	—	5.74	—	—
p-Cl	100	3.20	12.1	14.0	25
	80	2.65	9.51	13.5	27
	70	2.12	7.98	14.0	26
	60	1.53	5.74	14.0	26
	50	—	3.95	—	—
p-NO_2	100	36.7	135	11.1	30
	80	22.4	66.9	11.6	30
	70	16.5	49.6	11.6	30
	60	10.7	33.4	11.9	30
	50	—	19.4	—	—

$\Delta H^{\ddagger}$ in kcal·mole^{-1}. $\Delta S^{\ddagger}$ in e.u.

electron-withdrawing substituents) at 25 °C were determined for EtOH–TFE mixtures and presented in Table 5. The ρ values obtained for MeOH–MeCN mixtures are given in Table 6.

Assuming separate ρ values for bond breaking ($\rho<0$) and bond formation ($\rho>0$),[15,17] we are led to conclude that the transition state structure in the solvolysis of benzoyl chlorides varies from one of bond-breaking dominant to

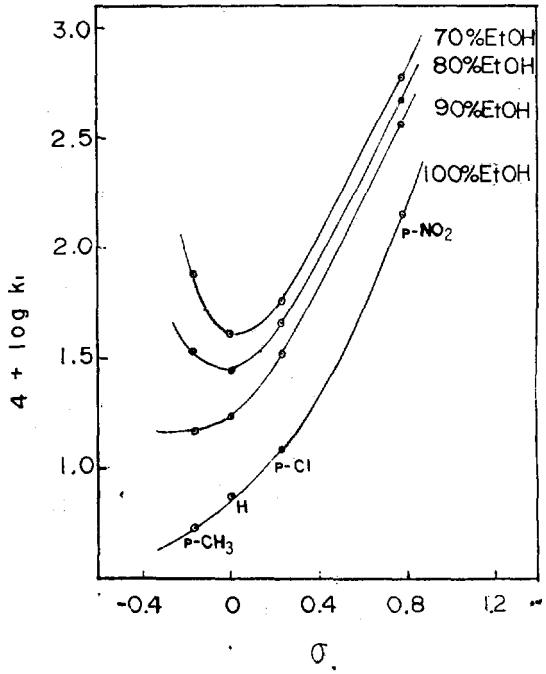

Figure 2. Hammett plot for the solvolysis of *para* substituted benzoyl chlorides in EtOH–H_2O mixtures at 25° C.

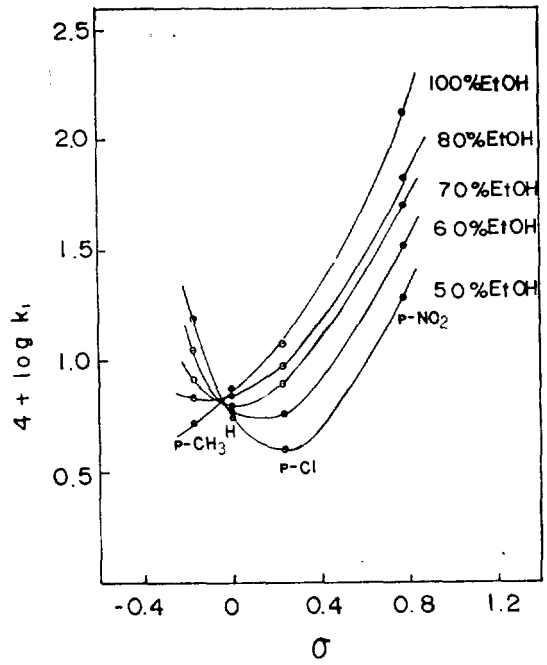

Figure 3. Hammett plot for the solvolysis of para substituted benzoyl chlorides in EtOH–TFE mixtures at 25 °C.

that of bond-making dominant on going from electron-donating substituents to those electron-withdrawing. A rate constant ratio defined as k_{solv}/k_E, where k_E is for ethanolysis, for rate constants obtained in EtOH–TFE mixtures (k_{solv}) are summarized in Table 7 and presented graphically as a plot of log (k_{solv}/k_E) *vs.* Y in Figure 4.

This figure illustrates the importance of bond-breaking with the electron-donating substituent and bond-making with the electron-withdrawing substituents. In Figure 5, a Grunwald–Winstein plot is presented for solvolysis in EtOH–TFE mixtures at 25 °C. For each substituent, a relatively good linear plot is obtained, from which approximate extrapolated rate constant for the pure TFE, k_T, was

TABLE 4: Rate Constants ($k_1 \times 10^3$ sec^{-1}) for the Methanolsis of *para* Substituted Benzoyl Chlorides in MeOH-MeCN Mixtures at 35 °C

MeOH (v/v %)	Substituents			
	p-MeO	*p*-CH_3	H	*p*-Cl
100	27.9	8.52	9.20	12.0
95	27.2	8.38	9.29	12.3
90	26.1	8.27	9.36	12.4
85	24.5	7.95	9.01	12.1
80	23.2	7.50	8.67	11.6
70	19.0	6.47	7.59	10.3
50	10.6	4.08	5.12	7.01

TABLE 5: ρ Values of Hammett Plot for the Solvolysis of *para* Substituted Benzoyl Chlorides in EtOH-TFE Mixtures at 25 °C

EtOH (v/v %)	ρ Value	
	ρ_1	ρ_2
100	0.91	1.51
80	0.07	1.30
70	−0.67	1.19
60	−1.58	1.02

TABLE 6: ρ Values of Hammett Plot for the Solvolysis of *para*-Substituted Benzoyl Chorides in MeOH-MeCN Mixtures at 35 °C

MeOH (v/v %)	ρ Value	
	ρ_1	ρ_2
100	−5.2	0.38
90	−5.0	0.43
80	−5.0	0.48
70	−4.7	0.56
50	−4.2	0.60

TABLE 7: Rate Constant for the Solvolysis of *para* Substituted Benzoyl Chlorides in EtOH-TFE Mixtures Relative to Those in EtOH

(a) 10 °C

Solvent, TFE (v/v %)	*p*-CH_3	H	*p*-Cl	*p*-NO_2
0	1.00	1.00	1.00	1.00
20	1.32	0.94	0.83	0.61
30	1.51	0.85	0.66	0.45
40	1.85	0.75	0.48	0.29

(b) 25 °C

Solvent, TFE (v/v %)	*p*-CH_3	H	*p*-Cl	*p*-NO_2
0	1.00	1.00	1.00	1.00
20	1.34	0.96	0.79	0.50
30	1.59	0.86	0.66	0.37
40	2.14	0.81	0.47	0.25
50	2.94	0.77	0.33	0.14

determined. The ratio of k_E/k_T in Table 8 indicates that in general bond-formation is advanced and bond-making becomes more important with the more electron-withdrawing substituent.

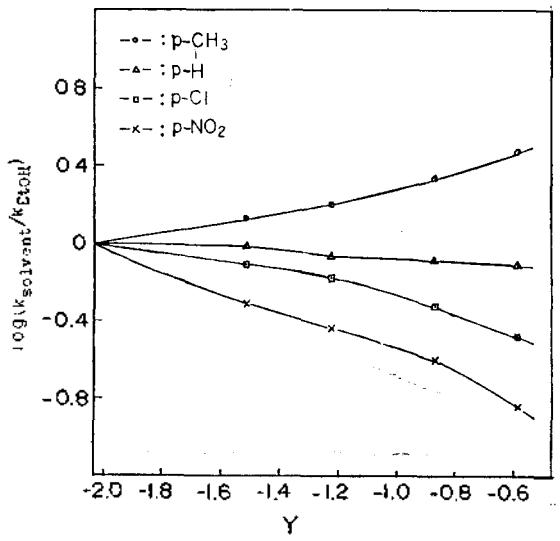

Figure 4. Variation in log ($k_{solvent}/k_{EtOH}$) at 25 °C with Y for the solvolysis of *para* substituted benzoyl chlorides.

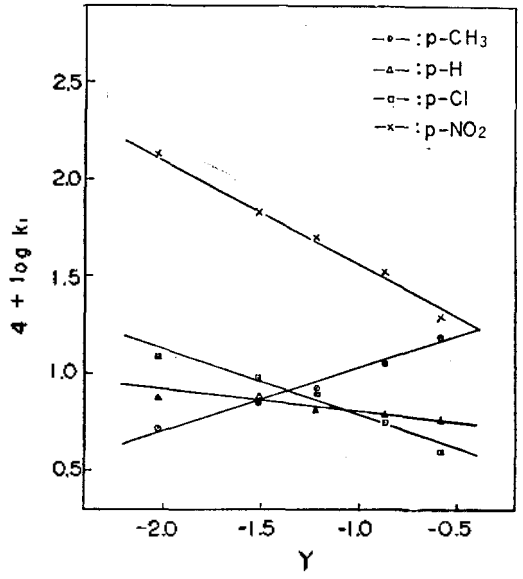

Figure 5. Grunwald-Winstein plots for the solvolysis of *para* substituted benzoyl chlorides in EtOH-TFE mixtures at 25 °C.

TABLE 8: Selectivity (k_E/k_T) for the Solvolysis of *para* Substituted Benzoyl Chlorides in EtOH-TFE Mixtures at 25 °C

p-CH_3	H	*p*-Cl	*p*-NO_2
0.1	2	6	120

The values of parameters m and l in eq.(1) are given in Table 9; it is evident that the l value, which is a measure of bond-formation[12], increases considerably whereas the m value, which is a measure of bond-breaking[12], decreases a little as the substituent changes to a more electron-withdrawing one. These values are useful in predicting the effect of substituent on the extent of bond-forming and bond-breaking in the transition states.

Transition State Variation. In this work, transition state variation with change of N and Y in eq. (4) are discussed.

TABLE 9: Derived Values of the Grunwald-Winstein Parameters *m* and *l* for the Solvolysis of *para* Substituted Benzyol Chlorides in EtOH-H_2O and EtOH-TFE Mixtures at 10 °C, 25 °C

(a) 10 °C

Substituents	m_E	m_T	m	l
p-CH_3	0.40 (r=0.995)	0.23 (r=0.999)	0.42	0.22
H	0.25 (r=0.999)	−0.11 (r=0.968)	0.28	0.48
p-Cl	0.15 (r=0.993)	−0.27 (r=0.974)	0.19	0.53
p-NO_2	0.14 (r=0.986)	−0.45 (r=0.997)	0.19	0.75

(b) 25 °C

Substituents	m_E	m_T	m	l
p-CH_3	0.43 (r=0.992)	0.32 (r=0.987)	0.44	0.14
H	0.28 (r=0.999)	−0.08 (r=0.976)	0.31	0.46
p-Cl	0.25 (r=0.985)	−0.33 (r=0.973)	0.30	0.74
p-NO_2	0.24 (r=0.993)	−0.56 (r=0.996)	0.31	1.03

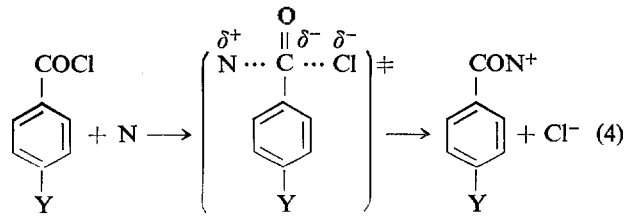

where N=EtOH, MeOH, TFE and H_2O, and Y=p-CH_3, H, p-Cl and p-NO_2.

Three possible paths for nucleophilic substitution process are shown in Figure 6: Path A(S_N2), path B(S_N1) and path C(S_AN). In the S_N2 process, N-R bond-making and R-X bond-breaking are synchronous and progressed to approximately the same extent, and hence little charge should be developed at the carbon center in the transition state.The S_AN process proceeds *via* an addition intermediate (N^+-R^--X) and the S_N1 via an intermediate (N R^+ X^-) in which bond-cleavage of RX is complete.

Let us consider types of reaction path expected from change of solvent and increase in electron-withdrawing ability of substituent. Increasing the TFE content of EtOH-TFE mixture has the effect of increasing ionizing power of solvent, and consequently will stabilize upper corners of the potential energy surface diagram in Figure 6. In this case, *anti*-Hammond effect[8] requires the transition state A on the S_AN path to move to D.

Experimentally this should cause the ρ_C value to decrease. Likewise Hammond effect requires B on the same S_AN path to move to G, which should cause an increase in the ρ_C value. On the other hand, the transition state C on the S_N2 path will move to J as a result of vecor sum of *anti*-Hammond and Hammond effects[4,7,8] Experimentally the ρ_C value should increase or decrease a little depending on the relative magnitude of the vectors I and H. Experimental results obtained in this work show a decrease in the ρ_C value with the increase of TFE content of the EtOH-TFE mixture.

Increasing electron-withdrawing power of substituent should stabilize the lower right corner of the potential energy surface diagram (Figure 6) and the transition state A should move to E (Hammond effect) leading to a decrease in l and

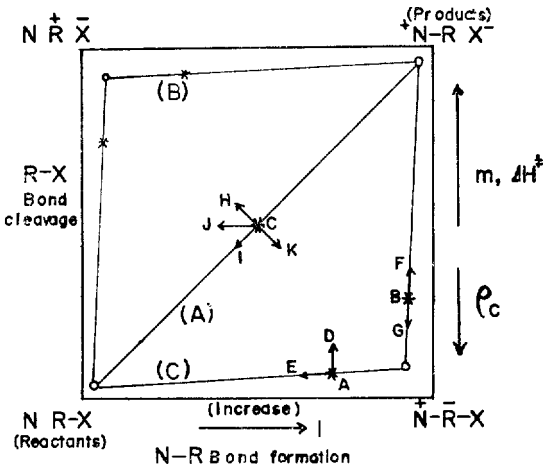

Figure 6. A PES plot for a nucleophilic displacement reaction, where N is the nucleophile, X is the leaving group, and minima and maxima are represented by circles and star marks, respectively. Path A, path B and path C represent the reaction coordinates for an S_N2, S_N1 and S_AN reactions, respectively.

little change in m and ΔH^* experimentally. The transition state B will similarly move to *F* leading to little change in l and increase in m and ΔH^*. On the other hand, C will move to K leading to an increase in l and a decrease in m and ΔH^* experimentally. Actual experimental results obtained in this work are the increase of l and decrease of m and ΔH^* with increasing electron-withdrawing ability of substituent. The predicted and observed changes of ρ_C, m, l, and ΔH^* values are summarized in Table 10. This table indicates that reaction coordinate appropriate for the reaction studied is a diagonal one, *i.e.*, S_N2 process. There are three positions of transition state possible along this diagonal reaction

TABLE 10: Summary of Prediction for the Different S_N Reaction Coordinate

	↑ X_{TFE} Lower upper corners			↑ σ_e^- (Increase of E.W. ability) Lower lower right corner					
		Prediction	Observed		Prediction			Observed		
		ρ_C	ρ_C		m	l	ΔH^*	m	l	ΔH^*
→	↑	−		←	0	−	0			
↗	↗ ↘	±	−	↘	−	+	−	−	+	−
↑	↓	+		↑	+	0	+			

TABLE 11: Summary of Predictions for Different S_N2 Transition State for *R* with Electron-Withdrawing Substituents

Parameters	Prediction			Observed
	Early(A)	Midway(B)	Late(C)	
m, ΔH^* (Degree of bond cleavage)	No change	Lower	Higher	Lower
l (Degree of formation)	Lower	Higher	No change	Higher
k_E/k_T (Degree of formation)	Lower	Higher	No change	Higher

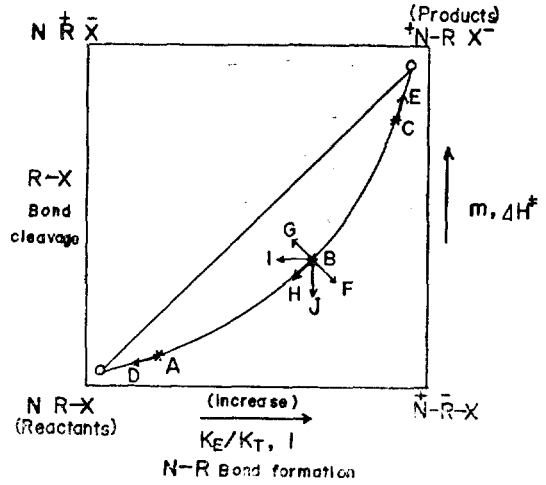

Figure 7. A PES plot for an S_N2 process in which N–R bond formation precedes R-X bond cleavage. Energy minima and maxima are shown as open circles and star marks, respectively.

coordinate: early (A), midway(B) and late(C) transition state. Adopting a similar procedure (Table 11), to that used for nucleophilic substitution reaction of benzensulfonyl derivatives by us,[6] we are led to a midway transition state (B) as the most suitable one for the solvolysis of benzoyl chlorides in EtOH–TFE mixtures.

Let us now compare transition state variation predicted from the potential energy surface model with those from the quantum mechanical model for the nucleophilic substitution reaction of benzoyl derivatives. Increasing the ionizing power of solvent has the effect of stabilizing X^- anion and will lower the upper corners of the potential energy surface (Figure 7); vector sum of the two effects, *anti*-Hammond and Hammond effects, should then move B to I. In other words, increasing the ionizing power by increasing TFE and water content in EtOH–TFE and EtOH–H_2O respectively stabilizes X^- ion, which causes the transition state B to move to I. The new transition state I has a looser N–R bond with little charge transfer from N to R and essentially unchanged R–X bond.

Quantum mechanically, the increase in the ionizing power leads to the stabilization of BA* configuration in which electrons are already largely localized on the leaving group.[9] The stabilized BA* will lead to an increase in the amount of BA* configuration in the transition state. This, in turn, is expected to have a bond-loosening effect on the N–R and R–X bonds (Table 1). Experimental results show a decrease in ρ_C and an increase in ΔH^* values. The decrease of ρ_C suggests a decrease in the N–R bond formation whereas the increase of ΔH^* suggests an increase in the R–X bond cleavage in the transition state.[16] The transition state structure derived from the experimental results is therefore a loose one in agreement with that predicated from the quantum mechanical model. If the stabilization of the leaving group X through the increase in the ionizing power of solvent had larger effect on the perpendicular component (*anti*-Hammond effect) than the parallel component (Hammond effect), the vector G would be relatively larger than the vector *H*, and a new vector sum will be oriented in a direction of increasing R–X bond cleavage. This will lead to a looser N–R and R–X bonds in agreement with experimental results.

Increasing the methanol content of MeOH–MeCN mixture should increase the nucleophilicity of the solvent; on the potential energy surface, Figure 7, this will lead to the transition state movement from B to J, since right hand corners of the diagram are stabilized. The effect will be to decrease the R–X bond cleavage with little change in the N–R bond. Quantum mechanically it will manifest as an increase of B^+A^- configuration in the transition state. Reference to Table 1 suggests that a tighter N–R and a looser R–X bond in the transition state will result. Experimentally a decrease in ρ and an increase in k_1 were observed with the increase of MeOH content. Since we would expect a smaller ρ value if bond-breaking ($\rho<0$) proceeded concertedly with bond-formation ($\rho>0$)[17] the experimental result of decreasing ρ with the increase of MeOH content is an indication that the "push-pull" type of mechanism[18] is operating more efficiently with the increase of MeOH content; the prediction of the quantum mechanical model of a tight N–R and a loose R–X transition state is therefore in line with the experimental results.

Electron-donating substituents will move the transition state B to G according to the potential energy surface model in Figure 7, which will lead to a looser N–R and R–X bond. On the other hand, electron-withdrawing substituents cause B to move to F, and a new transition state with a tighter N–R and R–X bond will be formed.

Quantum mechanically, however, and electron-donating substituent stabilized the BA* and destabilizes the B^+A^- configuration, whereas the BA configuration is little affected. The predominant contribution of BA* will give a looser transition state. An electron-withdrawing substituent should stabilize the B^+A^- configuration and will give a transition state with a tighter N–R and a looser R–X bond. In this case, however, the three electron bond R–X has the two resonance valence-bond(VB) structures,[9] R: ·X and R· :X, the former VB structure being more stabilized by the electron-withdrawing substituent. This increases the coupling with R· :X, resulting in the strong R–X bond[9]. This, in turn, leads to a tight R–X bond. On the basis of this qualitative argument, we can conclude that little change in R–X will occur as a result of the opposing effects.

Experimental results in Table 9 show that an increase in the *m* accompanied by a decrease in the *l* value are observed with the more electron-donating substituent, while little change in the *m* accompanied by an increase in the *l* value are observed with the more electron-withdrawing substituent. In view of the fact that the *m* is a mesaure of the extent of bond (R–X) breaking whereas the *l* is that of bond (N–R) formation, the experimental results are in full accord with the predictions of quantum mechanical model but are only in partial accord with those of the PES model.

We are thus led to recognize the superior nature of the quantum mechanical model in the prediction of transition state variation for the solvolysis of benzyoyl derivatives.

Conclusions

(i) the potential energy surface model of predicting transition state structure suggests an S_N2 mechanism, where bond-formation is somewhat more important, for the solvolysis of benzoyl chlorides.

(ii) Transition state variation predicted with the quantum mechanical model is consistent with the experimental results whereas the predictions provided by the potential energy surface model is found to be inconsistent in some cases.

Acknowledgement. We are grateful to the Ministry of Education and the Korea Science and Engineering Foundation for support of this work.

References

(1) (a) I. Lee and H. W. Lee. *J. Korean Nuclear Soc.*, **7**, 311 (1975); (b) R. F. Hudson and G. W. Loveday, *J. Chem. Soc.*, 766 (1966); (c) R. Fuchs and A. Nisbet, *J. Amer. Chem. Soc.*, **81**, 2371 (1959); (d) J. B. Hyne and R. Will, *ibid.*, **85**, 3650 (1963).

(2) P. R. Young and W. P. Jencks, *J. Amer. Chem. Soc.*, **101**, 3288 (1979).

(3) F. L. Schadt, T. W. Bentley, and P. V. R. Schleyer, *ibid.*, **98**, 7667 (1976).

(4) J. M. Harris, S. G. Shafer, J. R. Moffatt, and A. R. Becker, *ibid.*, **101**, 3296 (1979).

(5) R. A. More O'Ferrall, *J. Chem. Soc.(B)*, 274 (1970).

(6) I. Lee, I. S. Koo and H. K. Kang, *Bull. Korean Chem. Soc.*, **2**, 41 (1981).

(7) G. S. Hammond, *J. Amer. Chem. Soc.*, **77**, 334 (1955).

(8) E. R. Thornton, *ibid.*, **89**, 2915(1967).

(9) (a) S. S. Shaik, *ibid.*, **103**, 3692 (1981).
(b) A. Porss and S. S. Shaik, *ibid.*, **103**, 3702 (1981).

(10) (a) J. N. Murrell, M. Randic and D. R. Williams, *Proc. Roy. Soc.*, **A284**, 566 (1965); (b) T. Fueno, S. Nagase, K. Tatsumi and K. Yamaguchi, *Theoret. Chim. Acta*, **26**, 43 (1972); (c) K. Fukui and H. Fujimoto, *Bull. Chem. Soc. Jpn.*, **41**, 1989 (1968).

(11) I. Lee, K. S. Koh and S. La, *J. Korean Chem. Soc.*, **24**, 1 (1980).

(12) I. Lee and I. S. Koo, *ibid.*, **25**, 7 (1981).

(13) E. G. Guggenheim, *Phil. Mag.*, **2**, 538 (1926).

(14) L. M. Mukherjee and E. Grunwald, *J. Phys. Chem.*, **62**, 1311 (1958).

(15) I. Lee, K. B. Rhyu and B. C. Lee, *J. Korean Chem. Soc.*, **23**, 277 (1979).

(26) O. Rogne, *J. Chem. Soc.(B)*, 1294 (1969).

(17) (a) L. P. Hammett, "Physical Organic Chemistry," p. 184 ff McGraw-Hill Book Co., New York, 1940; (b) H. H. Jaffe, *Chem. Revs.*, **53**, 191 (1953).

(18) C. G. Swain and C. B. Scoot, *J. Amer. Chem., Soc.*, **70**, 119, 2289 (1948); **73**, 2813 (1951); **77**, 3731 (1955).

The Effect of Hybridized Atomic Orbitals of Ligands on the Calculated Dipole Moments for Octahedral [M(III)O_3S_3] Type Complexes

Sangwoon Ahn† and Eui Suh Park

Department of Chemistry Jeoubug National University, Jeonju 520, Korea

Chang Jin Choi

Department of Chemistry, Won Kwang University, Iri 510, Korea *(Received January 13, 1982)*

Extended Hückel calculations have been performed to obtain molecular orbital energies and the corresponding eigenvectors for [M(III)O_3S_3] type complexes{M(111) =V(111), Cr(III), Mn(III), Fe(III) and Co(III)} adopting the valence basis set orbital (nP_z) and the hybridized atomic orbital of ligands. The effects of the hybridized atomic orbital of ligands on the calculated dipole moments and 10 D_q values are investigated. The calculated 10 D_q values and dipole moments are close to the experimental values when the hybridized atomic orbital of ligands is used to obtain the eigenvector for [M(III)O_3S_3] type complexes.

Intoduction

A great deal of interest has been concentrated on physical measurements of infrared, electronic, nmr and esr spectra, magnetic moments and dipole moments of transition metal [M(III)O_3S_3] type complexes to obtain their structual information.[1]

In the previous works, we have reported the calculated dipole moments for octahedral [M (III)O_3S_3] type complexes by using σ-bonding molecular orbitals and valence bond